Calculated Schwoebel barriers on Si(111) steps using an empirical potential

S. Kodiyalam, K. E. Khor and S. Das Sarma
Department of Physics, University of Maryland, College Park, Maryland 20742-4111
(Received 14 July 1995)

Motivated by the recent investigations on instabilities caused by Schwoebel barriers during growth and their effects on growth or sublimation by step flows, we have investigated, using the Stillinger-Weber potential, how this step edge barrier arises for the two high symmetry steps on 1×1 reconstructed Si(111). Relative to a barrier of 0.97 ± 0.07 eV on the surface, we find additional (Schwoebel) barriers of 0.61 ± 0.07 eV and 0.16 ± 0.07 eV for adatom migration over the $[\bar{2}11]$ and the $[1\ 12]$ steps, respectively. The adatom potential energy is found to be strongly correlated with that derived from the local geometry of atoms on the adatom-free surface or step edges. This correlation preserves a strict correspondence between the barrier determining features in the spatial variation of the adatom potential energy and the same derived from the local geometry for the Si(111) surface and the $[\bar{2}11]$ step. It is therefore argued that the Schwoebel barrier on the $[\bar{2}11]$ step is robust, i.e., a feature that would survive in more satisfactory *ab initio* or tight binding calculations. Using a diffusion equation for the adatom concentration, the relevance of the barrier to electromigration of steps has been explored. Data from such experiments on Si(111) has been used to place an upper bound on the Schwoebel barrier and a lower bound on the electromigration force.

I. INTRODUCTION

The Schwoebel barrier was originally introduced in the context of step motion[1] as the additional barrier for adatom diffusion over a step edge from the upper to lower terraces. It was argued that such a barrier results in an anisotropy in adatom diffusion into the step edge — the diffusion from the lower terrace being greater. This anisotropy was found to drive an arbitrary distribution of step spacings towards a uniform distribution during growth of a vicinal surface.[1] Later, it was pointed out by Villain[2] that this growth by step flow is stable only on a sufficiently vicinal surface with possible instabilities setting in during the growth of a flat (singular) surface. The dynamical morphology of a singular surface growing under the influence of a schwoebel barrier is a subject of great current activity.[3–7] While the eventual fate of growth on a flat surface in the presence of such extra step-edge barriers is still being discussed,[3–7] it is now well accepted that Schwoebel barriers lead to coarsening in the evolving surface morphology under nonequilibrium growth conditions, producing mounds, pyramids, and facetlike angular structures on the growing surface. Recent experimental studies of nonequilibrium growth on the Si(111) surface have produced somewhat contradictory[8–10] results, and the specific role of Schwoebel barriers for nonequilibrium Si(111) growth is unclear at the present time.

The current study is primarily motivated by observations of another instability: As was pointed out by Schwoebel and Shipsey,[1] an anisotropy favoring diffusion into the step edge from the upper terrace (possibly due to larger barriers for diffusion from the lower terrace) results, in a step pairing instability, during the growth of a vicinal surface. In recent experiments similar direct-current induced reversible step-bunching instabilities have been observed during sublimation of the high temperature 1×1 phase of Si(111).[11,12] Here, we report on a calculation of the Schwoebel barrier for the two high symmetry vicinal steps on 1×1 Si(111), using the empirical Stillinger-Weber potential.[13] The importance of the Schwoebel barrier in the context of the electromigration experiments has also been explored by modeling the barrier as affecting the boundary conditions to the diffusion equation for adatom concentration used to interpret these experiments.[14]

II. EMPIRICAL POTENTIAL CALCULATIONS

The use of the Stillinger-Weber potential in this study has been motivated by its successful application in previous studies of bulk and liquid silicon,[13] the Si(100) surface and steps on this surface.[15] Barriers on the Si(100) surface and on single and double height steps on this surface have also been calculated using this potential.[16–18] Although this potential fails to reproduce the correct energetics of the Si(111) surface configurations with adatoms,[19] it has been used here since features that follow purely from the changes in the adatom coordination number are expected to be robust, i.e., these features survive even if the details of the empirical potential used change. Such features are expected to survive in more satisfactory *ab initio* or tight binding calculations. The calculation here is followed by an attempt to identify such robust features.

To determine the diffusion barriers the adatom potential energy has been mapped as a function of the (x,y) position of the adatom [in the (111) plane] for the Si(111) surface [Fig. 1(a)], the $[\bar{2}11]$ step [Fig. 1(d)] and the $[1\ 12]$ step [Fig. 1(g)]. The threefold and reflection symmetry of the Si(111) as shown in Fig. 2 implies that steps running along directions with equal θ are identical. It has been shown in a previous study[20] using the Stillinger-Weber potential that an alternative configuration of step-edge atoms with some of the upper terrace atoms rebonding to atoms in the lower terrace gives a lower step energy for the $[1\ 12]$ and $[101]$ steps. However, such a configuration has not been considered here since it has also been shown that it gives rise to step-step

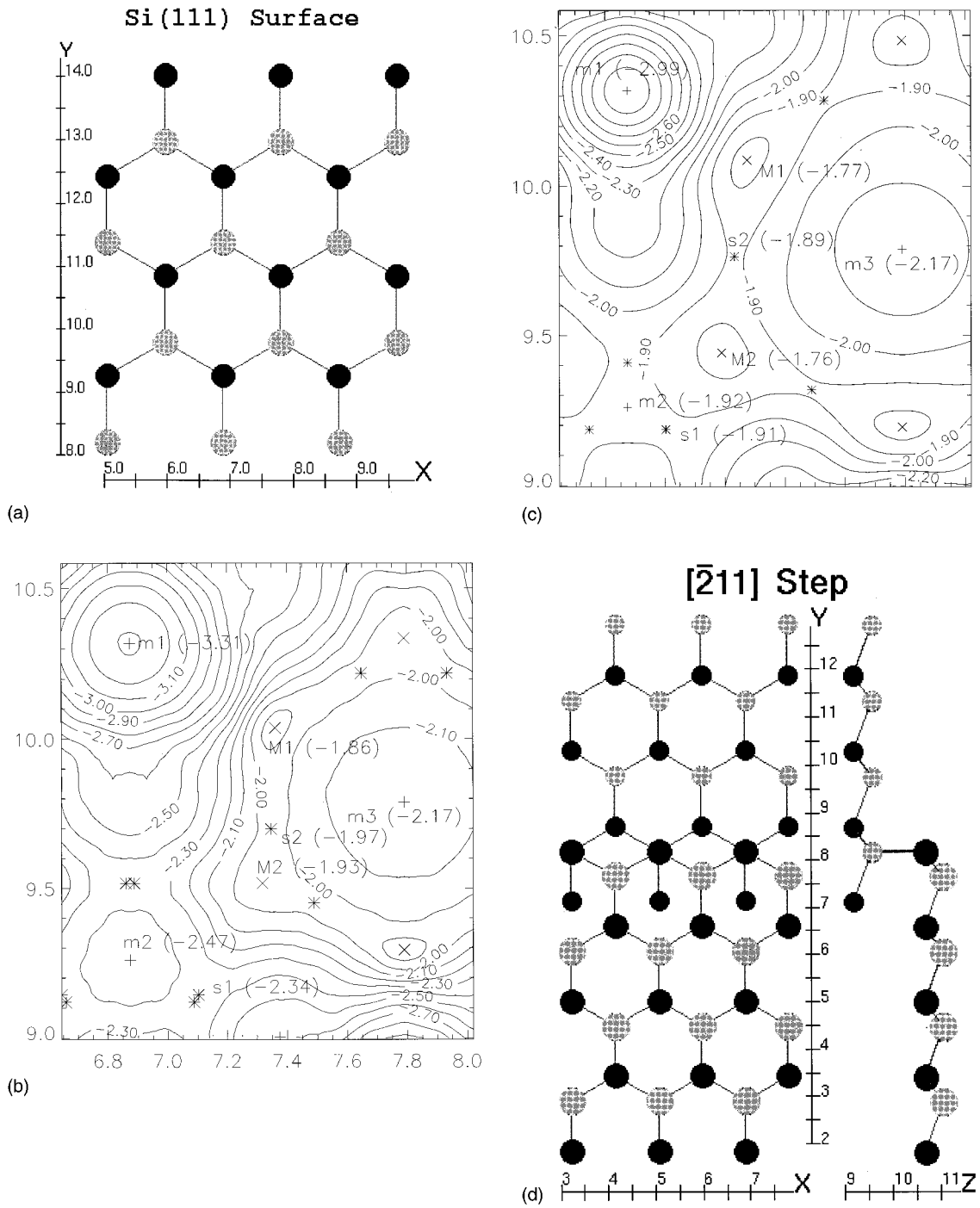

FIG. 1. The Si(111) surface (a) (the upper monolayer is shown in gray and the lower monolayer in black), the $[\bar{2}11]$ step (d), and the $[1\,\bar{1}2]$ step (g) (for the step configurations the upper bilayer is shown with larger atoms as compared to the lower bilayer). (b), (e), and (h) show the corresponding adatom binding energy $V(x,y)$. (c), (f), and (i) show the corresponding binding energy derived from the local geometry $V_{\rm lg}(x,y)$. Minima, saddle points and maxima are marked (labeled) by $+(m)$, $*(s)$, and $\times(M)$, respectively, with the figure in parentheses being their corresponding value in eV. In (b) and (c) the contours are 0.1 eV apart. In (e), (f), (h), and (i), they are 0.2 eV apart. In (e) and (h), contours of $V \geqslant -2.2$ eV and in (f) and (i), those of $V_{\rm lg} \geqslant -1.9$ eV are marked with dashed lines. The contour plots suggest a strong correlation between V and $V_{\rm lg}$. The diffusion barrier on the surface is determined by $m1$ and $s1$ in (b) and (c). The Schwoebel barrier is determined by $s3$ in (e) and (f), whereas it is determined by $s5$ in (h) and $s6$ in (i). There is a one-to-one correspondence between the barrier determining features in $V(x,y)$ and $V_{\rm lg}(x,y)$ for the Si(111) surface and the $[\bar{2}11]$ step, suggesting that the Schwoebel barrier on the $[\bar{2}11]$ step is a robust feature.

interactions an order of magnitude larger than experimental estimates.[20] Neglecting such rebonded configurations, all the intermediate low symmetry steps ($0° < \theta < 60°$) have been shown to have a higher step energy.[20] In other words, diffusion barriers have been calculated for those steps, the interactions of which are not larger than experimental estimates

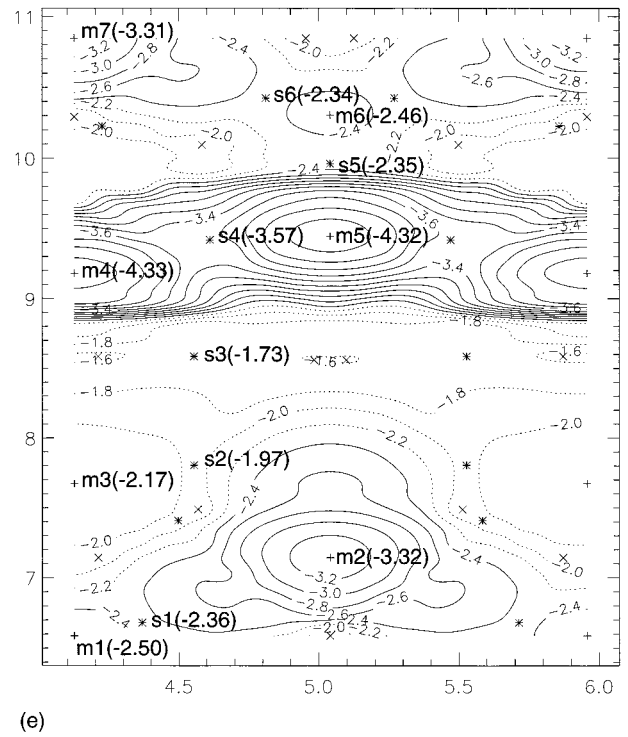

(e)

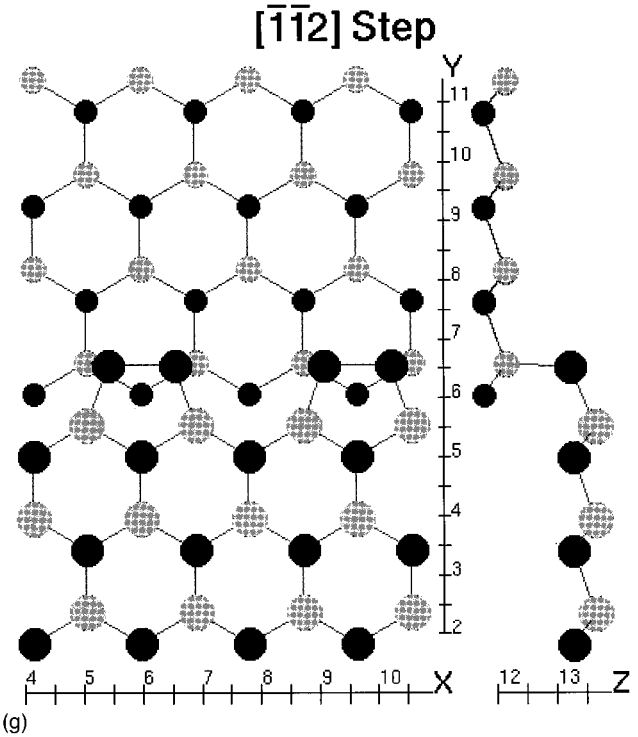

(g)

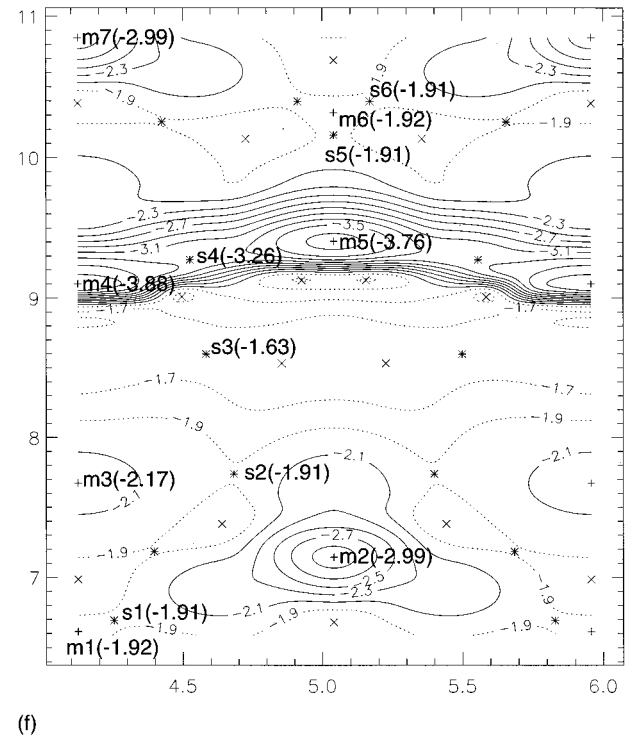

(f)

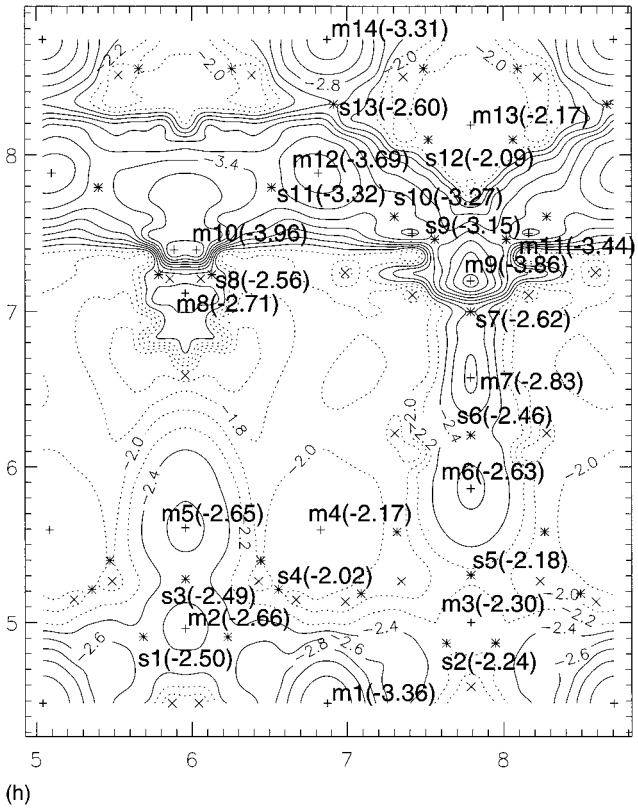

(h)

FIG. 1 (*Continued*).

and whose step energy is a local minimum as a function their orientation θ. The adatom potential energy V has been computed as the difference in the minimum potential energy of the system with the adatom at infinity (noninteracting) and the same with the interacting adatom.

Standard molecular dynamics (MD) procedures of integrating Newton's law (with dissipation to reduce temperature) and the steepest descent equations have been used to determine the minimum potential energy of the system.[20] These routines determined the adatom potential energy to an accuracy of 10^{-4} eV. The (x,y) coordinates of the adatom are fixed during the integration process. The system consisted of a certain number of bi-layers of Si(111) in an MD cell, with the surface lattice constants a_1 and a_2 along its x

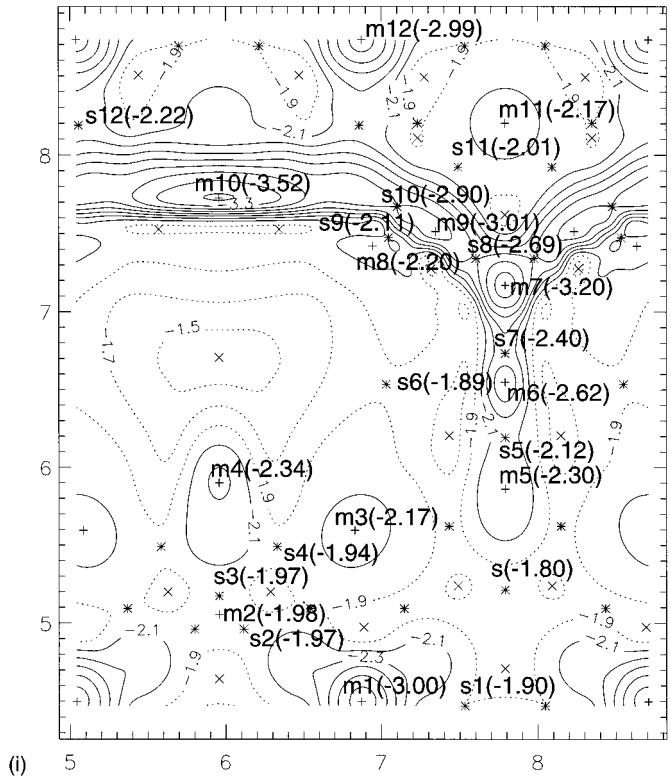

FIG. 1. (*Continued*).

and y directions, respectively (see Fig. 2). Three of the bottom bilayers are fixed at bulk lattice coordinates throughout the calculation. In simulations on the Si(111) surface, with six additional (movable) bilayers, it was found that changing the adatom's (x,y) position from a deep minimum lead to the shearing of the entire surface in the xy plane towards the adatom. As this made the (x,y) position of the adatom relative to the surface ill defined, further simulations on the surface as well as the step configurations were carried out with atoms at the (x,y) boundaries also fixed at positions corresponding to the adatom free but relaxed configurations. The regions in the (111) plane explored in all cases were ''centrally'' located, i.e., maximally away from the boundaries, so that finite size effects are minimized. System size dependence in $V(x,y)$ was initially explored for the Si(111) surface to determine the optimal system size. It was found that changing the system size from four lattice constants in the x and y directions (including the boundary of fixed atoms) with three movable bilayers to six lattice constants in the x and y directions with six movable bilayers changed (reduced) the adatom potential energy (at the minima, maxima, and saddle points) by $<10^{-2}$ eV. As an error bar of $\pm 10^{-2}$ eV was estimated to be smaller than the accuracy needed for this study, all the simulations were carried out with the smaller system size — the size in the y direction being extended to $4\frac{2}{3}$ and $4\frac{1}{3}$ lattice constants for the $[211]$ and $[1\ 12]$ step configurations, respectively, so that periodic boundary conditions could be applied to create vicinal steps. Since the bulk terminated Si(111) surface and $[\bar{2}11]$ step configurations do not relax under the Stillinger-Weber potential, with the system sizes chosen here, their corresponding surface and step energies are reproduced exactly. However, the $[1\ 12]$ step configuration is different from the bulk terminated structure, due to the 2×1 reconstruction at the step edge. With the system size chosen, here it's step energy is reproduced to within 4×10^{-4} eV/a_1.[20]

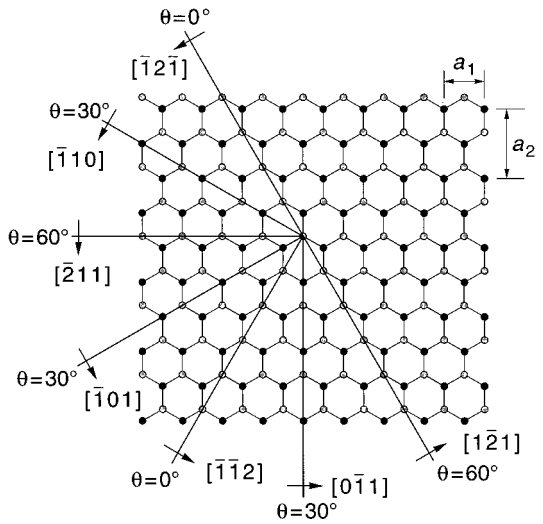

FIG. 2. One bilayer of the Si(111) surface consisting of the upper monolayer (gray) and lower monolayer (black). The figure shows the threefold and reflection symmetry of this surface: Steps running along directions with equal θ are identical. (Borrowed from Ref. 20.)

The MD procedures began with initial configurations for each (x,y) position of the adatom, corresponding to the relaxed adatom-free structures. The z coordinate of the adatom was chosen to be equal to that obtained in the final configuration, during simulation with the adatom in the immediate neighborhood of the point (x,y). For the step configurations, $V(x,y)$ was determined from behind to the front of the step edge. These procedures for determining $V(x,y)$ were found necessary for the $[\bar{2}11]$ step configuration, since other methods such as an arbitrary initial z coordinate for the adatom or determining $V(x,y)$ from the front to behind the step edge lead to the adatom relaxing into configurations in which it displaces an atom near the step edge and/or moves into the bulk. Symmetries in the (111) plane were exploited to reduce the size of the regions in which the adatom potential energy needs to be computed. Therefore, for the Si(111) surface, only a sixth of the surface unit cell was explored. For this case, $V(x,y)$ was computed on a triangular grid — the sides of the triangle coinciding with the high symmetry directions with the distance between neighboring grid points being $a_2/9$. An interpolation scheme respecting the symmetries on the surface was used to determine the features of $V(x,y)$. For the $[\bar{2}11]$ and $[1\ 12]$ step configurations, reflection symmetry about the y axis ($\perp$ to the step edge) reduced the width of the region (along the step edge) explored to a length of $a_1/2$ and a_1, respectively. For these configurations, $V(x,y)$ was determined on a rectangular grid with the distance between neighboring grid points being $a_1/16$ and $a_2/30$ along the x and y axis, respectively. With the step edge in the middle, the length of the region explored was $1\frac{2}{3}a_2$ and $1\frac{1}{3}a_2$ for the $[\bar{2}11]$ and $[\bar{1}12]$ steps, respectively. This

was to enable an interpolation scheme (respecting the symemetries of the step configurations) applying periodic boundary conditions along the x axis to do the same along the y axis of the region explored. On comparing the potential energy of the adatom on the Si(111) surface to that far away from the $[\bar{2}11]$ step-edge errors due to the finite grid sizes, the interpolation schemes and possibly effects due to being close to the boundary of fixed atoms were recognized. These errors are conservatively estimated to be ± 0.05 eV. Since this is much larger than the errors, due to finite size effects, it is assumed to be the error bar in the potential energy. Barrier values, which are differences in these potential energies, are therefore estimated to have an error bar of ± 0.07 eV.

III. RESULTS AND DISCUSSION

The results are shown in Fig. 1. The global minimum of the adatom potential energy V occurs on the H_3 site (m_1) on the Si(111) surface [Fig. 1(b)], where the adatom potential energy is -3.31 eV. This is a significant fraction of the bulk energy per atom: -4.34 eV. The relevant saddle point for $H_3 \leftrightarrow H_3$ transitions is s_1 (close to the T_4 cite, which is a local minimum), where the potential energy is -2.34 eV. Thus, the barrier to diffusion on the surface is 0.97 ± 0.07 eV. These results are consistent with previous studies (using the same potential) on surface energies of configurations with adatoms,[19] as well as a study of diffusion on the Si(111) surface.[21] The barriers to diffusion between the minima along the step edges are slightly smaller than the barrier on the surface — apparently inconsistent with previous work,[22] showing that step-edge fluctuations are (predominantly) due to attachment/detachment of adatoms from the terrace and not due to diffusion of atoms along the step edge. In this study, the Schwoebel barrier has been defined to be the difference between the maximum adatom potential energy (along the path on which this is a minimum), as it moves into the step edge from the global minimum on the upper terrace, far away from the step edge and the same for the $H_3 \leftrightarrow H_3$ transitions on the Si(111) surface. In other words, it is the difference in the adatom potential energies at the barrier determining saddle point on the step configurations and the same on the free surface (s_1). With this definition the Schwoebel barrier cannot be negative. From Fig. 1(e) [Fig. 1(h)], for the $[\bar{2}11]$ ($[1\ \bar{1}2]$) step 1, the barrier is determined by s_3 (s_5), where the adatom potential energy is -1.73 eV (-2.18 eV)—implying a Schwoebel barrier of 0.61 ± 0.07 eV (0.16 ± 0.07 eV). Growth on Si(111) is, therefore, expected to produce moundlike structures with facets consisting (predominantly) of $[\bar{2}11]$ steps. However, the experiments of Yang *et al.* (temperature $= 275 \pm 5\,^{\circ}$C) instead show facets with $[1\ \bar{1}2]$ steps.[9] This discrepancy may be due to the presence of the 7×7 reconstruction.

It must be noted that the Stillinger-Weber potential has been tuned only to the properties of the bulk diamond and liquid structures of silicon and not to any surface or step properties. As mentioned previously, it does not produce the correct energetics for the Si(111) surface configurations with adatoms[19] as compared to *ab initio* calculations.[23–25] Therefore, an attempt has been made to identify the robust features of this study: Features following from changes in the coordination number of the adatom. This idea is supported by the observation that the reconstruction energy of the Si(100) surface calculated using the Stillinger-Weber potential[26] (0.85 eV) agrees with *ab initio* calculations[27] (0.84 eV). The Tersoff and Dodson empirical potentials also give this energy as the same order of magnitude.[26] The Stillinger-Weber also reproduces the correct order of energies of the $[\bar{2}11]$ and $[1\ \bar{1}2]$ steps (per step-edge atom, these values are 0.72 eV and 0.62 eV, respectively[20]), as well as the presence of rebonding at the $[1\ \bar{1}2]$ step edge, as compared to tight binding calculations (per step edge atom these values are 0.70 eV and 0.38 eV, respectively[28]). During reconstruction, the coordination number of atoms (on the (100) surface and $[1\ \bar{1}2]$ step edge) changes from two to three. It is, therefore, expected that features following from such a change in coordination number are not artifacts of the empirical potential used. Here, the adatom energy recomputed *without additional* relaxation of other atoms, due to the presence of the adatom, is assumed to be a good measure of the coordination number. Although this measure is very similar to the actual adatom energy $V(x,y)$, it helps to identify features that follow from the geometry of atoms (locally around to adatom) on the relaxed adatom-free surface or step edges. Features that do not change significantly, due to additional relaxations in the presence of the adatom, are expected to be robust. The adatom potential energy $V_{lg}(x,y)$ has therefore been recomputed with other atoms fixed at positions corresponding to the relaxed adatom-free structures. These results are shown in Fig. 1(c) for the Si(111) surface, Fig. 1(f) for the $[\bar{2}11]$ step, and in Fig. 1(i) for the $[1\ \bar{1}2]$ step. Similarities in the contour plots of V and V_{lg} suggest a strong correlation between them. This correlation is evident from the linear relationship between V_{lg} and V (Fig. 3) The lines in Fig. 3 are best fits to $V_{lg}(x,y)$ vs $V(x,y)$, which were explicitly computed at the grid points. There is no repetition of points that are equivalent, due to the symmetries of the relevant configurations.

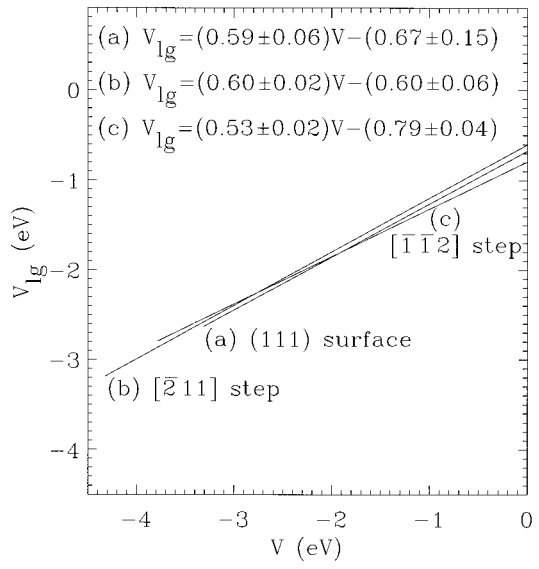

FIG. 3. Plots of the adatom potential energy derived from the local geometry of fixed atoms V_{lg} vs the actual adatom potential energy V. The straight line fits show the strong correlation between V_{lg} and V. The rough configuration independence of the relationship suggests that it is a characteristic of the (111) surface.

Further, for the step configurations, the length of the region along the y axis corresponding to these plots is $1/2a_2$ on either side of the step edge. The rough configuration independence of the relationship between $V_{\rm lg}$ and V suggests that it is a characteristic of the [111] surface. A similar behavior may be true for the Si(100) surface and single height steps on it. In this case, borrowing the values of V corresponding to the features (minima and saddle points) from previous work by Roland and Gilmer,[16–18] and computing $V_{\rm lg}$ for the same features here, it is found that $V_{\rm lg}=(1.3\pm0.2)V+(1.2\pm0.5)$ for the Si(100) surface and $V_{\rm lg}=(1.1\pm0.1)V+(0.6\pm0.3)$ for the combined data from the three single height steps.

A. Relevance to electromigration experiments

Recent experiments on the electromigration of steps on Si(111) (Refs. 11 and 12) can be reinterpreted in the presence of a Schwoebel barrier, by modifying the boundary conditions to the diffusion equation for adatom concentration used previously by Stoyanov *et al.*[14] to describe step bunching (see Appendix A). This particular modification is to suppress the strength of the step as a source of adatoms onto the upper terrace relative to the same onto the lower terrace by a factor e^{ϵ}, where $\epsilon=2E_s/k_bT$, with E_s being the Schwoebel barrier. With this modification, the equations for adatom concentration on a particular terrace has four length scales — the diffusion length λ and the scale introduced by the electromigration force f $(=F/k_bT)$, both of which are parameters entering the diffusion equation and two other scales t_0 and t_1 entering the boundary condition to this equation at the upper and lower terrace step edges, respectively $(t_{0,1}=\beta_{0,1}/a^2Dn_e$, a^{-2} is the density of atoms in a terrace, D is the diffusion constant, n_e is the equilibrium adatom density, and β is the step kinetic coefficient — here the Schwoebel barrier is modeled as making this parameter assume different values at the upper and lower terrace step edges). These are, in addition to the scale, introduced by the terrace width W. Since the modification is further designed to keep the total strength of the step as a source of adatoms a constant independent of E_s, $t_0+t_1=t$ — a constant independent of ϵ for fixed k_bT (the variation of t with E_s is included in the estimated range of t), with $t_0/t_1=e^{\epsilon}$. The (linear) diffusion equation is then solved, with n_e appearing in the boundary conditions as a ''source,'' to obtain the spatial variation of the adatom concentration.

Using the above solution, the equations for the velocities of an array of steps with positions X_i are developed — the step index i increases in the step down direction, which is also the positive x axis. The time scale that enters these equations is the lifetime of an adatom $\tau_{\rm lf}$. These equations have the following form (see Appendix A):

$$\dot{X}_n=\frac{\theta_e}{\tau_{lf}}\lambda[g_-(\epsilon,t\lambda,f\lambda,W_n\lambda^{-1})+g_+(\epsilon,t\lambda,f\lambda,W_{n-1}\lambda^{-1})], \tag{1}$$

where $\theta_e=n_ea^2$ and the terrace width $W_n=X_{n+1}-X_n$. From the above, equations for the rate of change of the terrace widths can be obtained. Linear stability analysis of these equations around an average terrace width w would predict when the step-bunching instability occurs. The linearized equations may be written as follows:

$$\dot{\delta}_n=k_-\dot{\delta}_{n+1}+(k_+-k_-)\dot{\delta}_n+k_+\dot{\delta}_{n-1}, \tag{2}$$

where $\delta_n=W_n-w$ and $k_\pm=(\theta_e/\tau_{\rm lf})\lambda[\partial g_\pm/\partial W]_{W=w}$. The instability occurs if[29] $k_+-k_->0$ or equivalently (since $k_++k_-<0$, for $w>0$), when the anisotropy ratio $\rho=(k_+/k_-)<1$. This analysis is similar to the work of Ghez *et al.*,[30] which includes an external flux with the electromigration force being absent.

The recent experiment of Williams *et al.* on *reversible* step bunching on Si(111), which measures an ''effective'' anisotropy ratio $\rho_{\rm eff}$ (near bunched steps) in the temperature range 1155–1215 °C (this range includes the corrections, due to the emissivity of the optical pyrometer, used in the experiment[12]), can now be used to determine an upper bound on E_s (E_s^u) and a lower bound on F (F_l), by solving the equation $\tau^{-1}=k_+-\rho k_-=0$. The solution to this equation is obtained by estimating the parameters w, t, and λ (in the temperature range of interest: 1155–1215 °C and then determining f as a function of ϵ. The estimates of the upper and lower bounds on t and λ are made *conservatively* — the range is made wide enough so as to include the ''true value.'' Experimental observations of Latyshev *et al.*[11] show that around a temperature of 1200 °C, the step velocity varies linearly with the terrace width upto a width of 2 μm. A lower bound on the diffusion length[31] of 0.5 μm is obtained by reproducing this result using Eq. (1). This estimate is robust against large changes in the parameters t and f. To make this estimate, ϵ is conservatively chosen to be zero. Further, to first order in $w\lambda^{-1}$, $g_++g_-=-w\lambda^{-1}$ — independent of t, ϵ, and f. Therefore, the magnitude of the slopes of the above curves correspond to the evaporation rates $r=\theta_e/\tau_{lf}$. An estimate of the upper bound on λ is obtained by estimating the diffusion constant[31] D [using $D=b^2\nu e^{-E_a/k_bT}$, $b=3.84$ Å, $\nu=10^{13}$ s^{-1}, $E_a=0.97$ eV (calculated here)] and an estimate of the upper bound on $\tau_{lf}=n_ea^2/r$. [The temperature dependence of r in the data from Latyshev *et al.*[11] is consistent with the theory of Burton *et al.*[32] (BCF), with an activation energy equal to the cohesive energy of silicon ($E_b=4.34$ eV).] The upper bound on θ_e is *assumed* to be 0.167 — the primary motivation for this is that it is measured to be $\approx$ 0.1 around 900 °C and[33] its activation energy E_n, which is equal to E_b-E_τ (E_τ is the activation energy for τ_{lf}^{-1}) from the BCF theory, is estimated to be negative, since total energy calculations[34] predict smaller surface energies for silicon surfaces with adatoms as compared to the 1×1 surface thereby making $E_\tau>E_b$. The specific value of 0.167 is chosen as it corresponds to the density in any $\sqrt{3}\times\sqrt{3}$ configuration of adatoms, wherein all the floating bonds on the 1×1 substrate are saturated by bonding with the adatoms — at higher densities adatom interactions are *expected* to be significant. This bound is, therefore, required here as a measure of internal consistency in the analysis, since the diffusion equations used correspond to free adatoms. The upper bound on $\tau_{\rm lf}$ is calculated using this value of θ_e. As the variation in n_e has been argued to be small,[31] $E_n\approx0$ and $E_\tau\approx E_b>E_a$. The estimate of the upper bound on λ $(=(D\tau_{\rm lf})^{1/2})$ is, therefore, made at the lowest temperature of interest and is equal to $\approx$ 70 μm. The upper bound used in this study is $\approx$7 times this value, making $0.5\ \mu{\rm m}\leqslant\lambda\leqslant0.5\times10^3\ \mu$m.

The estimate of the range of t is obtained from the range of λ, the measured $r(T_2)$ (Ref. 11) and $\theta_e(T_1)$ (Ref. 33), and the relation between $\beta_s=\beta_0+\beta_1$ and the measured step mobility $\Gamma(T_1)$ (Ref. 22) (T_1 corresponds to 900 °C and T_2 corresponds to temperatures of interest). At the same temperature, $\beta_s=\Gamma/a^2$ (see Appendix B). From a model of attachment-detachment at the step edges (see Appendix B), the temperature and θ_e dependences of β_s is determined:

$$\beta_s \propto \frac{(e^{-2E_a/k_bT}+e^{-2(E_a+E_s)/k_bT})\,\theta_e^2}{1-\theta_e}.$$

The upper bound on β_s is derived using the above dependence from the lower bound $=\Gamma(T_1)/a^2$ ($E_a=0.97$ eV, E_s is set equal to a value that gives the largest increase). The parameter t is then evaluated using $t=\beta_s/a^2Dn_e$. This gives upper and lower bounds on t:

$$t_{u,l}=\frac{\Gamma(T_1)}{a^2\lambda^2 r(T_2^+)} \times\left(1,\frac{r(T_2^+)[1-\theta_e(T_1)]}{r(T_2^-)[1-\theta_e(T_2^+)]}\,\frac{[e^{-E_a/k_bT_2^+}T_2^+\theta_e(T_2^+)}{e^{-E_a/k_bT_1}T_1\theta_e(T_1)}\right]^2,$$

where T_2^+ (T_2^-) corresponds to the highest (lowest) temperature in the range of interest. The values of $r(T_2^+)$ and $r(T_2^-)$ are obtained from the data of Latyshev *et al.*[11] using $E_b=4.34$ eV, $\Gamma(T_1)$ from a previous measurement of Bartelt *et al.*,[22] $E_a=0.97$ eV, $\theta_e(T_1)=0.1$ (measured by Yang *et al.*[33]), and $\theta(T_2^+)=0.167$ (as assumed previously). This results in $7.7\times10^3\ \mu\text{m}/\lambda^2\leqslant t\leqslant 7.7\times10^3\ \mu\text{m}/\lambda^2\times10^{3.1}$. The range of t, therefore, depends on the value of λ.

The value of the parameter w used here is equal to the average terrace width in the experiment of Williams *et al.*[12] ($=0.15\ \mu$m), who determine ρ_{eff} to be 0.20 ± 0.03. It must be noted that the extraction of ρ from the experiment had used a theory[35] which makes $\rho_{\text{eff}}=\rho(w\lambda^{-1}=0)$ (w was much smaller than the average terrace width since, in the theory used, it corresponded to the distance between bunched steps). In this study, it is assumed that $\rho_{\text{eff}}=\rho(w\lambda^{-1}\neq0)$ — this may be a *reasonable* approximation since, here, $\lambda_{\min}=0.5\ \mu$m and the $W_{\max}$ in the experimental data used to determine ρ_{eff} was as large as $0.6\ \mu$m. This approximation is motivated by the need to study the solution of $\tau^{-1}=0$, including the full nonlinearity in $w\lambda^{-1}$.

The procedure for determining E_s^u and F_l assumes that an electromigration force F causes the step-bunching instability ($\rho=0.2$) with $-F$ restoring the stability ($\rho\geqslant1$). This assumption is motivated by the observation[12] that a current in the step up direction causes the step bunching, whereas an equal magnitude in the step down direction results in uniformly spaced steps. E_s^u and F_l are determined by studying the solutions to $\tau^{-1}=0$ (fixing t, λ, and w) for $\rho=0.2$ and $\rho=1.0$. The variation of τ^{-1} with F (with typical values of t, λ, w, E_s, and ρ) is shown schematically in inset (a) of Fig. 4. Of interest is the solution that exists even in the limit $w\lambda^{-1}=0$ (the other two solutions do not exist in this limit). The variation of this solution with E_s (fixed t, λ, and w) for $\rho=0.2$ and $\rho=1.0$ is shown schematically in inset (b) of Fig. 4. The two curves show that beyond a certain value of E_s, a force $-F$ (with F resulting in $\rho=0.2$) cannot restore stability. This value is, therefore, the upper bound (E_s^u) on E_s. Below E_s^u, the magnitude of F needed for $\rho=0.2$ is larger. The value of F at E_s^u is, therefore, the lower bound (F_l) on F. $F_0=F(E_s=0,\rho=0.2)$.

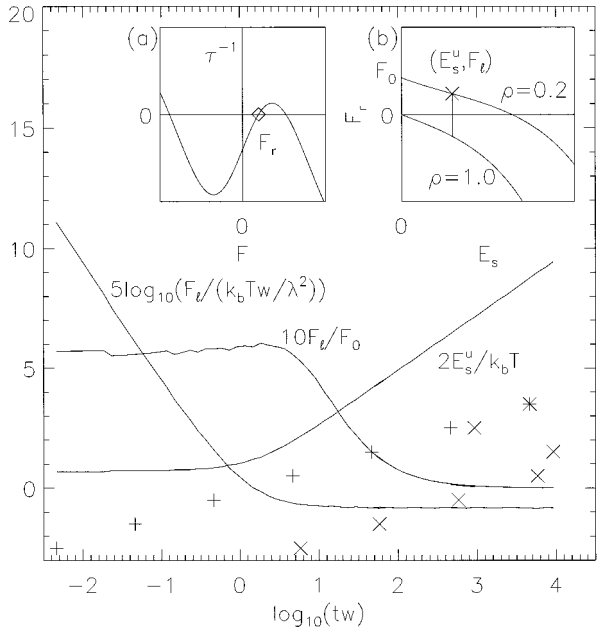

FIG. 4. Inset (a) shows schematically the variation of $\tau^{-1}=k_+-\rho k_-$ with F. The solution to $\tau^{-1}=0$ (of interest) is F_r, which exists even in the limit $w\lambda^{-1}=0$, whereas the other two do not. Inset (b) shows schematically the variation of F_r with E_s for $\rho=1.0$ and $\rho=0.2$. The upper bound on E_s (E_s^u) is determined from the condition $F(E_s>E_s^u,\rho=1.0)<-F(E_s\geqslant E_s^u,\rho=0.2)$. It can be seen that $F(E_s^u,\rho=0.2)$ is the lower bound on F (F_l). $F_0=F(E_s=0,\rho=0.2)$. For the curves shown, $w=0.15\ \mu$m, $0.5\ \mu\text{m}\leqslant\lambda\leqslant0.5\times10^3\ \mu$m (seven values equally spaced on the logarithmic scale), with the range of t depending on λ: $7.7\times10^3\ \mu\text{m}/\lambda^2\leqslant t\leqslant7.7\times10^3\ \mu\text{m}/\lambda^2\times10^{3.1}$ ($\lambda>7\ \mu$m). The upper (lower) limits of t are marked by $+$ ($\times$). For $\lambda<7\ \mu$m, the upper limit of t is forced to be smaller than that estimated, since the solution F_r ceases to exist. For $\lambda<1\ \mu$m, F_r does not exist for even the smallest t. This shows that $\lambda_{\min}=1\ \mu$m. For $w\lambda^{-1}\to0$, $E_s^u=0.35k_bT=0.05$ eV (for the experiment in Ref. 12)—significantly less than that calculated here for the $[\bar{2}11]$ step (0.61 ± 0.07 eV). This suggests that $[1\,1\,\bar{2}]$ steps were observed.

Figure 4 shows the variation of F_l, E_s^u, and F_0 with the parameters t and λ ($w=0.15\ \mu$m). As noted previously, the range of the t depends on the value of λ, with additional restrictions on the upper bound of t. These restrictions are due to the absence of the solution (of interest) to $\tau^{-1}=0$ for small λ and large t. This seems to correspond the behavior observed at higher temperatures,[12] wherein a current in the step *down* direction causes the step bunching instability. For $tw\leqslant1$, the curves in Fig. 4 correspond to the limit $w\lambda^{-1}\to0$ and can be obtained by solving $\tau^{-1}=0$ to zeroth order in $w\lambda^{-1}$. This gives

$$F=\frac{k_bT}{\lambda^2 t}\left(\frac{(1+e^{-2E_s/k_bT})-\rho(1+e^{2E_s/k_bT})}{\rho-1}\right). \qquad (3)$$

Using the above expression, E_s^u, F_l, and F_0 are found to be

$$E_s^u = \frac{k_b T}{2} \ln\left(\frac{3+\rho_0}{3\rho_0+1}\right), \tag{4}$$

$$F_l = \frac{k_b T}{\lambda^2 t}\left(\frac{4(1-\rho_0^2)}{(3+\rho_0)(3\rho_0+1)}\right), \tag{5}$$

$$F_0 = \frac{k_b T}{\lambda^2 t}\left(\frac{2(1-\rho_0)}{1+\rho_0}\right), \tag{6}$$

with $\rho_0 = 0.2$ (here). Equation (4) gives $E_S^u = 0.05$ eV for the experiment of Williams *et al.*[12] This is much smaller than the barrier calculated here for the $[\bar{2}11]$ step (0.61 ± 0.07 eV), suggesting that $[1\,1\,\bar{2}]$ steps were seen in the experiment. From Eq. (6) and the electric field in the experiment[12] (700 V/m), the (maximum) charge needed on the adatoms [in units of the (negative) electronic charge] is estimated to be reasonably small—in the range 3×10^{-2} to $3\times10^{-5.1}$. From Fig. 4, it can be seen that with a Schwoebel barrier the charge needed is always smaller than with a zero barrier. For $tw > 1$, the deviation of the curves from the above expressions is significant — this is due to the dependence of τ^{-1} on $w\lambda^{-1}$, which requires that terms of order $w\lambda^{-1}$ and higher be considered. In this range, the minimum charge needed on the adatoms (using F_l) continues to have a reasonable lower limit as it is in the range 2×10^{1} to 7×10^{-5}.

IV. CONCLUSIONS

In summary, the adatom potential energy contours have been calculated for the 1×1 reconstructed Si(111) surface and the two high symmetry single height steps on it using the empirical Stillinger-Weber potential. From these plots, diffusion barriers along the path of minimum barrier height can be calculated for transitions between any two minima. The results show that barriers for diffusion in the trench along the step edge are smaller than that between that global minima on the free surface. There is also a strong correlation between that adatom potential energy and the potential energy derived from the local geometry of atoms on the adatom-free surface or surface or Si(111) surface (0.97 ± 0.07 eV) and the Schwoebel barrier on the $[\bar{2}11]$ step (0.61 ± 0.07 eV) are robust features, due to changes in adatom coordination number. Interpreting recent electromigration experiments in the presence of a Schwoebel barrier shows that smaller values of electronic charge on the adatoms can account for the observations. It also suggests, in the limit where the diffusion length (λ) is much larger than the terrace width (w), that $[1\,1\,\bar{2}]$ steps were observed in the experiment.[12] However, this conclusion relies on assumptions regarding the nature of the atomic processes at the step edge [that these processes may involve two atoms (at a kink site) which see the barriers as computed here] and that $w\lambda^{-1} \to 0$. Future studies addressing these assumptions may interpret electromigration experiments differently.

ACKNOWLEDGMENTS

One of the authors (S.K.) wishes to thank E.D. Williams, N.C. Bartelt, Elain Fu, D.J. Liu, D. Kandel, and S.V. Khare for useful discussions. This work has been supported by the NSF-MRG and the U.S. ONR.

APPENDIX A: ANALYSIS OF THE DIFFUSION EQUATION FOR STEP MOTION

The diffusion equation for noninteracting adatoms subliming in the presence of an electromigration force F perpendicular to the step edge and the absence of an external flux may be written in the ''adiabatic approximation'' (which neglects the time derivative of the density) as follows:[14,30]

$$\frac{d^2 n}{dx^2} - f\frac{dn}{dx} - \frac{n}{\lambda^2} = 0, \tag{A1}$$

where n is the density of adatoms, $f = F/k_b T$, λ is the diffusion length, and the positive x axis coincides with the step down direction. This equation can be solved using the boundary conditions on the current j ($= D[-dn/dx + fn]$, where D is the diffusion constant). These conditions determine the step velocity V [$= a^2(-j_l + j_u)$, where a^2 is the inverse terrace density, j_u is the current towards the step edge from the upper terrace, and j_l is the current away from the step edge on the lower terrace] and define the step kinetic coefficient β. In the presence of a Schwoebel barrier (E_s), this parameter is modeled as assuming the values β_0 and β_1 at the upper ($x = 0$) and lower ($x = W$) terrace step edges, respectively, with $\beta_0/\beta_1 = e^{\epsilon}$, where $\epsilon = 2E_s/k_b T$. The boundary conditions can now be written as follows:

$$\left[-\frac{dn}{dx} + fn\right]_{x=0} = -\frac{te^{\epsilon}}{1+e^{\epsilon}}[n(0) - n_e],$$

$$\left[-\frac{dn}{dx} + fn\right]_{x=W} = \frac{t}{1+e^{\epsilon}}[n(W) - n_e], \tag{A2}$$

where n_e is the equilibrium density and $t = (\beta_0 + \beta_1)/a^2 D n_e$. The solution to the diffusion equation under the above boundary conditions is shown below:

$$n(x) = n_e(Ae^{W\lambda^{-1}\eta_+} + Be^{W\lambda^{-1}\eta_-}), \tag{A3}$$

with

$$\eta_\pm = f\lambda/2 \pm \sqrt{[1 + (f\lambda/2)^2]},$$

$$A = \frac{\psi e^{W\lambda^{-1}\eta_-} - \varphi}{\phi\psi e^{W\lambda^{-1}\eta_-} - \varphi\chi e^{W\lambda^{-1}\eta_+}},$$

$$B = \frac{\phi - \chi e^{W\lambda^{-1}\eta_+}}{\phi\psi e^{W\lambda^{-1}\eta_-} - \varphi\chi e^{W\lambda^{-1}\eta_+}},$$

where

$$\phi = 1 - \frac{(\eta_+ - f\lambda)(1+e^{\epsilon})}{t\lambda e^{\epsilon}}, \quad \varphi = 1 - \frac{(\eta_- - f\lambda)(1+e^{\epsilon})}{t\lambda e^{\epsilon}},$$

$$\chi = 1 + \frac{(\eta_+ - f\lambda)(1+e^{\epsilon})}{t\lambda}, \quad \text{and} \quad \psi = 1 + \frac{(\eta_- - f\lambda)(1+e^{\epsilon})}{t\lambda}.$$

The velocity (V_n) of a particular step edge (X_n) can now be calculated:

$$V_n = a^2\{-j_l[=j(x=0,W=X_{n+1}-X_n)] + j_u[=j(x=W,W=X_n-X_{n-1})]\}.$$

From the functional form of the density and using $D=\lambda^2/\tau_{lf}$ (τ_{lf} is the lifetime of an adatom), it may be seen that

$$V_n = \frac{n_e a^2}{\tau_{lf}}\lambda(g_- + g_+), \tag{A4}$$

where $g_\pm$ are dimensionless functions of dimensionless arguments given by

$$g_-(\epsilon, t\lambda, f\lambda, W\lambda^{-1}) = t\lambda[e^\epsilon(A+B-1)/(1+e^\epsilon)],$$

$$g_+(\epsilon, t\lambda, f\lambda, W\lambda^{-1}) = t\lambda[(Ae^{W\lambda^{-1}\eta_+} + Be^{W\lambda^{-1}\eta_-} - 1)/1 + e^\epsilon],$$

with the symmetry $g_+(-a,b,-c,d) = g_-(a,b,c,d)$.

APPENDIX B: AN ATOMIC MODEL FOR THE STEP KINETIC COEFFICIENT

The step kinetic coefficient β was introduced by Chernov[36] through the supposition that the currents (j_l from the lower terrace and j_u from the upper terrace) towards a step edge (at $x=X$) are proportional to the deviation of the adatom density n in the neighborhood of the step from the equilibrium density n_e. From the model adopted here, it will be shown that, in the presence of a Schwoebel barrier, this parameter assumes different values, i.e., β_0 and β_1 determining j_l and j_u, respectively:

$$j_l = -\frac{\beta_0}{a^2}\left[\frac{\theta(X^+)-\theta_e}{\theta_e}\right], \quad j_u = \frac{\beta_1}{a^2}\left[\frac{\theta(X^-)-\theta_e}{\theta_e}\right], \tag{B1}$$

where $a^2 = 1/(\text{terrace density})$, $\theta = na^2$, and $\theta_e = n_e a^2$, with the positive x axis in the step down direction. These equations serve as the boundary conditions used in this work [Eq. (A2)].

The temperature dependence of β_0 (β_1) can be derived assuming an activated model for adatom attachment-detachment at the step edge from the lower (upper) terrace with the single atom activation barrier being E_a (E_a+E_s), where E_a is the barrier on the free surface and E_s is the Schwoebel barrier.[37] However, since silicon has two atoms in its unit cell, *successful* attachment-detachment processes at the kink sites of steps must involve two atoms. Single atom processes from energetically favorable step-edge configurations lead to unfavorable ones and are expected to have very large barriers. Further, the probability of simultaneous attachment (detachment) of two atoms is proportional to θ_e^2 [$(1-\theta_e)^2$]. The currents are, therefore, given by

$$j_l = -\frac{\nu_l e^{-2E_a/k_bT}\theta^2 - c_l(1-\theta)^2}{a_\parallel},$$

$$j_u = \frac{\nu_u e^{-2(E_a+E_s)/k_bT}\theta^2 - c_u(1-\theta)^2}{a_\parallel},$$

where $a_\parallel$ is the lattice constant along the step and $\nu_{l,u}$ are "effective" attachment attempt frequencies. The vanishing of these currents in equilibrium (when $\theta=\theta_e$) determine the constants $c_{l,u}$. Further assuming $\nu_l=\nu_u=\nu$ and neglecting terms of the order $(\theta-\theta_e)^2$, gives

$$j_l = -\frac{2\nu\theta_e e^{-2E_a/k_bT}}{a_\parallel(1-\theta_e)}(\theta-\theta_e),$$

$$j_u = \frac{2\nu\theta_e e^{-2(E_a+E_s)/k_bT}}{a_\parallel(1-\theta_e)}(\theta-\theta_e),$$

from which β_0 and β_1 can be identified. Hence,

$$\beta_0+\beta_1 = \frac{2\nu a^2}{a_\parallel}\left[\frac{\theta_e^2}{1-\theta_e}\right](e^{-2E_a/k_bT} + e^{-2(E_a+E_s)/k_bT}), \tag{B2}$$

$$\frac{\beta_0}{\beta_1} = e^{2E_s/k_bT}. \tag{B3}$$

Relationship between the step kinetic coefficient and the step mobility

To relate the step mobility Γ and the step kinetic coefficient $\beta_s=\beta_0+\beta_1$, the expression for the step velocity $[dX/dt = a^2(j_u - j_l)]$ must be obtained in terms of β_s.[38] From Chernov's defining equations (B1),

$$\frac{dX}{dt} = \frac{1}{\theta_e}[\beta_1\theta(X^+) + \beta_0\theta(X_-) - \beta_s\theta_e]. \tag{B4}$$

This equation needs to be extended to account for the two dimensional character of the step: The currents towards the step edge are proportional to the deviation of the chemical potential μ from the equilibrium chemical potential near the step edge μ_e^s. These relationships may be assumed to be the defining equations for the step mobilities Γ_1 and Γ_0:

$$j_u = \frac{\Gamma_0}{a^4}[\mu(X^-) - \mu_e^s], \quad j_l = -\frac{\Gamma_1}{a^4}[\mu(X^+) - \mu_e^s]. \tag{B5}$$

Assuming the existence of a coarse-grained free energy functional $\mathcal{F}$ of the step configuration $\{x(y)\}$, μ_s^e is given by Mullins[39] to be

$$\mu_e^s = \mu_e + \frac{a^2}{k_bT}\frac{\delta\mathcal{F}(x(y))}{\delta x}, \tag{B6}$$

where μ_e is the equilibrium chemical potential on the terrace far away from the step edge. Further adopting his model of a dissolving substance for the adatoms, and in an approximation in which the deviation of the density θ from the equilibrium density θ_e (the density far away from the step edge) is much smaller than θ_e, the chemical potential and the density can be related by[39]

$$\mu(\theta) - \mu_e = k_bT\frac{\theta-\theta_e}{\theta_e}. \tag{B7}$$

Using Eqs. (B6) and (B7), it can be seen that the equilibrium density beside the step edge is different from θ_e.[40–42] Further, using Eq. (15), the step velocity can be given by

$$\frac{\partial x}{\partial t}=\frac{1}{\theta_e}\left[\frac{\Gamma_1}{a^2}\theta(x^+)+\frac{\Gamma_0}{a^2}\theta(x^-)-\frac{\Gamma\theta_e}{a^2}\left(1+\frac{a^2}{k_bT}\frac{\delta\mathcal{F}(x(y))}{\delta x}\right)\right], \tag{B8}$$

where $\Gamma=\Gamma_0+\Gamma_1$. In the absence of an external force on the adatoms and when attachment-detachment of atoms from the terrace onto the step edge is rate limiting in relation to terrace diffusion, it is expected that $\theta(x^+)=\theta(x^-)=\theta_e$. Then, Eq. (B8) reduces to the Langevin equation (without the noise term ζ):[43,22]

$$\frac{\partial x}{\partial t}=-\frac{\Gamma}{k_bT}\frac{\delta\mathcal{F}(x(y))}{\delta x}+\zeta(y,t).$$

Within the small slope approximation ($\partial x/\partial y<<1$), $\delta\mathcal{F}(x(y))/\delta x\propto\partial^2x/\partial y^2$. The spatial average (over y, denoted by $\langle\rangle$) of this term vanishes, due to periodic boundary conditions. Identifying $\langle x\rangle$ with X, assuming that the density is independent of y, and approximating $\langle\theta(x)\rangle=\theta(X)$, Eq. (B8) (on spatial averaging) gives

$$\frac{dX}{dt}=\frac{1}{\theta_e}\left(\frac{\Gamma_1}{a^2}\theta(X^+)+\frac{\Gamma_0}{a^2}\theta(X^-)-\frac{\Gamma\theta_e}{a^2}\right). \tag{B9}$$

Equations (B4) and (B9) agree if

$$\beta_{0,1}=\frac{\Gamma_{0,1}}{a^2}\Rightarrow\beta_s=\frac{\Gamma}{a^2}. \tag{B10}$$

[1] R.L. Schwoebel and E.J. Shipsey, J. Appl. Phys. **37**, 3682 (1966).
[2] J. Villain, J. Phys. (France) I **1**, 19 (1991).
[3] M.D. Johnson, C. Orme, A.W. Hunt, D. Graff, J. Sudijono, L.M. Sander, and B.G. Orr, Phys. Rev. Lett. **72**, 116 (1994).
[4] M. Siegert and M. Plischke, Phys. Rev. Lett. **73**, 1517 (1994).
[5] A.W. Hunt, C. Orme, D.R.M. Williams, B.G. Orr, and L.M. Sander, Europhys. Lett. **27**, 611 (1994).
[6] I. Elkinani and J. Villain, J. Phys. (France) I **4**, 949 (1994).
[7] C.J. Lanczycki and S. Das Sarma, Phys. Rev. Lett. **76**, 780 (1996).
[8] J. Chevrier, A. Cruz, N. Pinto, I. Brebezier, and J. Derrien, J. Phys. (France) I **4**, 1309 (1994).
[9] H.N. Yang, G.C. Wang, and T.M. Lu, Phys. Rev. B **51**, 14 293 (1995)
[10] C.J. Lanczycki, Y.N. Yang, E. Fu, R. Kotlyar, E.D. Williams, and S. Das Sarma (unpublished).
[11] A.V. Latyshev, A.L. Aseev, A.B. Krasilnikov, and S.I. Stenin, Surf. Sci. **213**, 157 (1989).
[12] E.D. Williams, E. Fu, Y.N. Yang, D. Kandel, and J.D. Weeks, Surf. Sci. **336**, L746 (1995).
[13] F.H. Stillinger and T.A. Weber, Phys. Rev. B **31**, 5262 (1985).
[14] S.S. Stoyanov, H. Nakahara, and M. Ichikawa, Jpn. J. Appl. Phys. **33**, 254 (1993).
[15] T.W. Poon, S. Yip, P.S. Ho, and F.F. Abraham, Phys. Rev. Lett. **65**, 2161 (1990).
[16] C. Roland and G.H. Gilmer, Phys. Rev. Lett. **67**, 3188 (1991).
[17] C. Roland and G.H. Gilmer, Phys. Rev. B **46**, 13 428 (1992).
[18] C. Roland and G.H. Gilmer, Phys. Rev. B **46**, 13 437 (1992).
[19] X.P. Li, P.B. Allen, and J.Q. Broughton, Phys. Rev. B **38**, 3331 (1988).
[20] S. Kodiyalam, K.E. Khor, N.C. Bartelt, E.D. Williams, and S. Das Sarma, Phys. Rev. B **51**, 5200 (1995).
[21] K.E. Khor and S. Das Sarma, Chem. Phys. Lett. **134**, 43 (1987).
[22] N.C. Bartelt, J.L. Goldburg, T.L. Einstein, E.D. Williams, J.C. Heyraud, and J.J. Métois, Phys. Rev. B **48**, 15 453 (1993).
[23] J.E. Northrup and M.L. Cohen, Phys. Rev. B **29**, 1966 (1984).
[24] J.E. Northrup, Phys. Rev. Lett. **57**, 154 (1986).
[25] K.E. Khor and S. Das Sarma, Phys. Rev. B **39**, 1188 (1989).
[26] K.E. Khor and S. Das Sarma, Phys. Rev. B **36**, 7733 (1987).
[27] M.T. Yin and M.L. Cohen, Phys. Rev. B **26**, 5668 (1982).
[28] D.J. Chadi and J.R. Chelikovsky, Phys. Rev. B **24**, 4892 (1981).
[29] P. Bennema and G.H. Gilmer, in *Crystal Growth: An Introduction*, edited by P. Hartman (Elsevier, New York, 1973).
[30] R. Ghez, H.G. Cohen, and J.B. Keller, Appl. Phys. Lett. **56**, 1977 (1990).
[31] E. Fu (private communications).
[32] W.K. Burton, N. Cabrera, and F.C. Frank, Philos. Trans. R. Soc. London Ser. A **243**, 299 (1951).
[33] Y.N. Yang and E.D. Williams, Phys. Rev. Lett. **72**, 1862 (1994).
[34] R.D. Meade and D. Vanderbilt, Phys. Rev. B **40**, 3905 (1989).
[35] D. Kandel and J.D. Weeks, Phys. Rev. Lett. **74**, 3632 (1995).
[36] A.A. Chernov, Usp. Fiz. Nauk **73**, 277 (1961) [Sov. Phys. Usp. **4**, 116 (1961)].
[37] E.D. Williams (private communications).
[38] N.C. Bartelt (private communications).
[39] W.W. Mullins, in *Metal Surfaces*, edited by W.D. Robertson and N.A. Gjostein (American Society for Metals, Metals Park, OH, 1963), p. 17.
[40] N.C. Bartelt, T.L. Einstein, and E.D. Williams, Surf. Sci. **312**, 411 (1994).
[41] M. Uwaha and Y. Saito, Phys. Rev. B **68**, 224 (1992).
[42] G.S. Bales and A. Zangwill, Phys. Rev. B **41**, 5500 (1990).
[43] N.C. Bartelt, J.L. Goldburg, T.L. Einstein, and E.D. Williams, Surf. Sci. **273**, 252 (1992).